Aero-Acoustic assessment of installed propellers

Marius Gabriel COJOCARU*,[1], Mihai Leonida NICULESCU[1],
Mihai Victor PRICOP[1]

*Corresponding author
*,[1]INCAS – National Institute for Aerospace Research "Elie Carafoli"
B-dul Iuliu Maniu 220, Bucharest 061126, Romania
cojocaru.gabriel@incas.ro*, niculescu.mihai@incas.ro, pricop.victor@incas.ro

DOI: 10.13111/2066-8201.2015.7.2.5

3rd International Workshop on Numerical Modelling in Aerospace Sciences, NMAS 2015*,*
06-07 May 2015, Bucharest, Romania, (held at INCAS, B-dul Iuliu Maniu 220, sector 6)
Section 2 – Flight dynamics simulation

Abstract: *The volume of general aviation transport is increasing and consequently this gives rise to the need for reducing noise levels while improving or at least maintaining the same level of aerodynamic performance. This can be achieved through the use of modern propellers and engines. In this paper we present a methodology to study and predict the installed propeller noise at the same time with the aerodynamic characterization, through the use of unsteady CFD and Acoustic-Analogies analysis. The analysis shows the influence of different acoustic sources generated by the installed propeller on the far field noise by monitoring the monopoles and dipoles with and without taking into account the quadrupoles. In this way we can observe the influence of the distance from the propeller to the engine intake on the overall sound. Time averaged aerodynamic performances are presented along with instantaneous results.*

Key Words: *Aeroacoustic, CFD, Propeller, Ffowcs-Williams Hawkings, Direct Sound Computation.*

1. INTRODUCTION

The present paper presents a CFD method for computing the aerodynamic performances of a general aviation turboprop powered aircraft and its propeller. Then two aeroacoustic methods are presented for computing the noise levels, at far and near points, and the results are compared against each other. One method is based on the Direct Sound Computation within the CFD simulation while the other is based on the Ffowcs-Williams Hawkings acoustic analogy. Finally, the contribution to noise levels is analyzed for each noise source and the installation effects are summarized.

2. SOLVER SETTINGS AND MODELLING SIMPLIFICATIONS

Ansys - Fluent is a CFD software that has a very broad range of applications. The code uses the finite volume approach to discretize the Navier-Stokes equations (and their approximations Reynolds-Averaged Navier-Stokes, Large Eddy Simulation, etc.) and a wide array of related equations such as energy conservation, passive scalar transport equations, heat transfer, chemical reactions, noise propagation, etc. to solve the fluid flow and fluid flow related problems. This flexibility allows us to use Fluent to solve the compressible fluid flow around a propeller with nacelle and wing for aeroacoustic and aerodynamic purposes.

The assumptions made in the current computation are:

- The medium is considered to be a continuum.
- The flow is turbulent over the full domain.
- The equation of state is for an ideal gas.
- The flow is compressible.
- The equations are cast in the conservative form, and the solver is "density based", Roe method for flux discretization.
- The solution sought corresponds to an unsteady state.
- The influence of the fuselage on the flow field and noise scattering is minimal; therefore at the wing root a symmetry plane is introduced for the sake of simplicity.
- The chemical composition of the jet is identical to the air.
- Monopoles, dipoles and quadrupoles are accounted as acoustic sources.
- The airplane is in "climb after take-off" condition.
- The solver has a time-step in seconds chosen such that it that corresponds to 2°/time-step in propeller rotations.

Since we assume the flow to be governed by a compressible ideal gas at a fully turbulent regime in unsteady conditions we can use the URANS equations. The RANS approach is based on the k-ω STT turbulence model that uses the Boussinesq hypothesis.

This model was proposed by Menter and combines the advantages of traditional Low-Reynolds k-ω models near the wall with the classical k-ε models far from the walls, the two models are combined through blending functions.

This model has proved to be useful in computing flows in rotating domains and accurately predicting boundary layer separation and aerodynamic forces/moments for largely separated steady flows.

The equations are solved in the implicit approach and solution acceleration is made using the Algebraic Multi-Grid method.

Time integration is performed in the dual-time approach proposed by Jameson, and ensures the second order time accuracy. The existence of the Ffowcs – Williams Hawkings (FWH) model for predicting the far-field noise into Ansys Fluent allows us to perform the acoustic analysis.

Also the Ansys Fluent is able to perform Direct Sound Computation by monitoring the unsteady pressure fluctuations at specific locations; afterwards this data is transformed into Sound Pressure Levels (SPL) by using an adequate FFT (Fast Fourier Transform) solver.

The specific workflow for aeroacoustic computations is described hereafter:

1. The steady flow solution is computed in the specified regime, with the Multiple Reference Frame (MRF) method.
2. The unsteady solver is initialized with the steady flow solution and run for a number of at least 4 revolutions. The number of 4 full revolutions is obtained from experience in similar cases and is sufficient for the solver to "wash" away any unphysical solutions that arose from the initialization process. The MRF is changed into a sliding mesh method to model the propeller actual rotation.
3. Afterwards the FWH acoustic solver is switched on and monitoring for acoustic sources begins.
4. The unsteady solution is computed for another 2-3 full revolutions. The actual number of revolutions is calculated so that the acoustic perturbations have plenty of time to reach the locations where the sound is going to be measured.
5. The FHW acoustic analogy is performed for all the "microphone" locations.

Alternatively, for a Direct Sound Computation we set up monitoring points in the zone near the propeller and monitor there the unsteady pressure fluctuations. The pressure fluctuations are transformed in SPL and then corrected as if they were located on the surface of a sphere at 8 times the radius of the previous one.

The correction takes place in the following manner, for each doubling of the distance the SPL drops by 6dB.

The proof for this is very simple: let us assume that we have sound propagating as a spherical wave and we take a look at two instants, one at radius r_1 and one at r_2. The noise that generates this wave is characterized by the power P and at radius r_1 by the acoustic intensity $I_1 = P/4\pi r_1^2$ and at r_2 by $I_2 = P/4\pi r_2^2$.

By dividing them we get that $I_2/I_1 \sim r_1^2/r_2^2$, and knowing that $I \sim p^2$, we get that $p \sim 1/r$, where p stands for pressure.

Now by using the formula $SPL = 20log_{10}(p/p_0)$ (where p_0 is a reference pressure for sound traveling in air at normal conditions and is equal to $p_0 = 20\mu Pa$) we get that for the difference in: $SPL_2 - SPL_1 = 20log_{10}(p_2/p_1) = 20log(r_1/r_2 = 1/2) = 6.02dB$. Therefore for correcting for the sound on a sphere located at 8 ($=2^3$) times the radius of the previous one we simply get the SPL and subtract 18 ($=3 \cdot 6$).

3. GEOMETRY AND MESHING

Geometry and modeling assumptions and simplifications are given on short below:

- The flow inside the nacelle is ignored.
- All the nacelle's ventilation inlets/outlets are closed.
- The wing flap is ignored since there is no need to model the noise generated by it.
- The domain is split in a rotating part and a fixed one with respect to the reference frame.
- An exhaust jet domain is constructed to refine the mesh in that region.

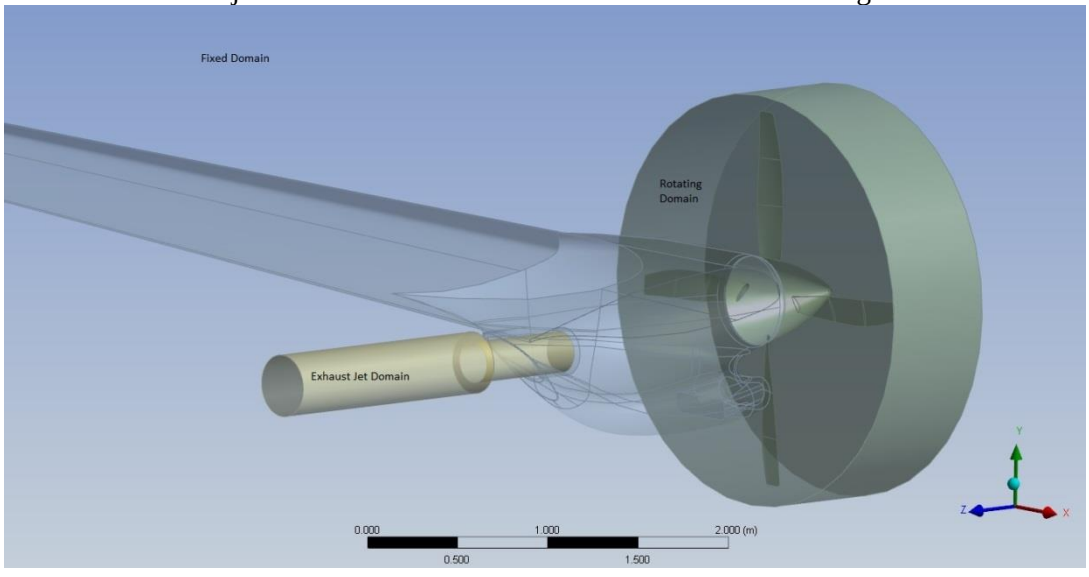

Fig. 1. – Geometry and computational domain

The mesh is constructed in Numeca's Hexpress and is based on a hexahedral volume-to-surface approach. The total number of elements is 18M cells for the fixed domain, 20M cells

for the rotor and 2M cells for the jet region.

The mesh was constructed as having a target of 25 Points-Per-Wavelength (PPW) in the rotor area near the blade and 23.5 PPW in the wake refinement region. The PPW cell size is based on the propeller Blade Passing Frequency (BPF) multipled by 5 that is estimated to be at 146.67·5 Hz and this leads to a propeller wavelength of $\lambda_{Propeler} = 0.46$m.

The factor of 5 comes from the fact that we are interested in monitoring at least 4 BPF accurately; this is why we chose to have a larger number of BPFs as reference frequency. The table with point coordinates where the "microphones" are placed is given.

For the radius of 1.2m (near field) the sound is computed directly from pressure fluctuations and for the radius of 9.6m, the sound is computed from FWH or by simply correcting the near field computed sound.

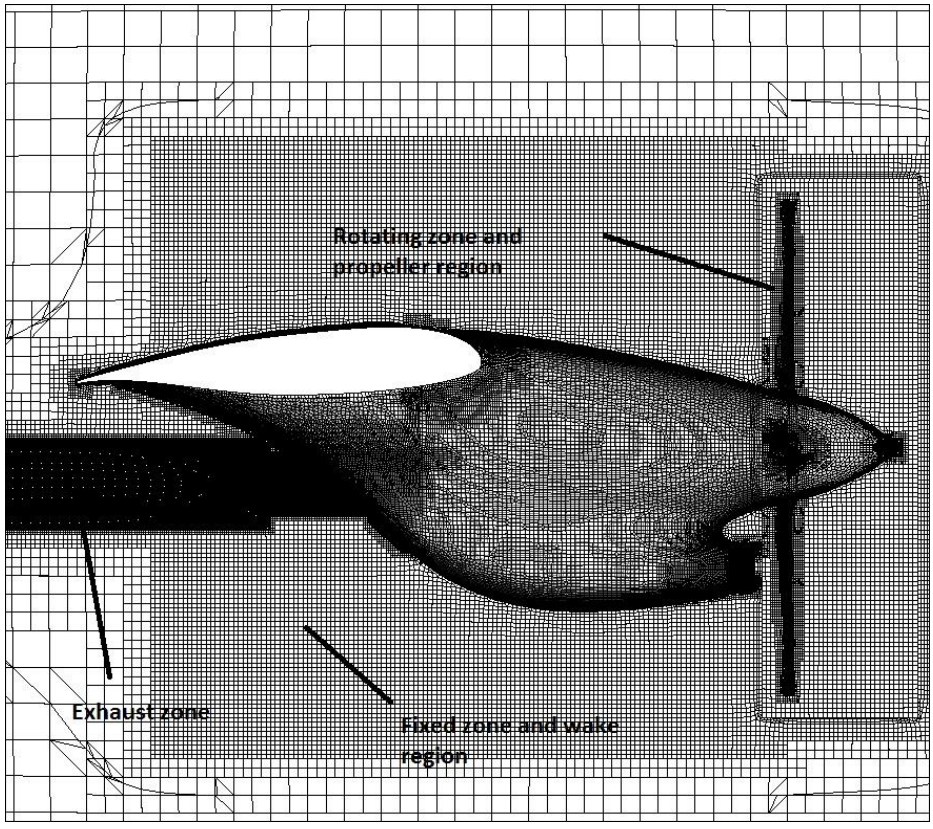

Fig. 2. – Mesh for the aerodynamic computations. Median plane

Deg.		Radius	x	y	z				Radius	x	y	z		
-90		1.2	0.000	0.000	-1.200	p1a	1		9.6	0.000	0.000	-9.600	p1d	11
-75		1.2	0.000	-0.311	-1.159	p2a	2		9.6	0.000	-2.485	-9.273	p2d	12
-60		1.2	0.000	-0.600	-1.039	p3a	3		9.6	0.000	-4.800	-8.314	p3d	13
-45		1.2	0.000	-0.849	-0.849	p4a	4		9.6	0.000	-6.788	-6.788	p4d	14
-30		1.2	0.000	-1.039	-0.600	p5a	5		9.6	0.000	-8.314	-4.800	p5d	15
-15		1.2	0.000	-1.159	-0.311	p6a	6		9.6	0.000	-9.273	-2.485	p6d	16
0		1.2	0.000	-1.200	0.000	p7a	7		9.6	0.000	-9.600	0.000	p7d	17
15		1.2	0.000	-1.159	0.311	p8a	8		9.6	0.000	-9.273	2.485	p8d	18
30		1.2	0.000	-1.039	0.600	p9a	9		9.6	0.000	-8.314	4.800	p9d	19
45		1.2	0.000	-0.849	0.849	p10a	10		9.6	0.000	-6.788	6.788	p10d	20
60									9.6	0.000	-4.800	8.314	p11d	21
75									9.6	0.000	-2.485	9.273	p12d	22
90									9.6	0.000	0.000	9.600	p13d	23

Fig. 3. – Locations of points in the near field (left) and far field (right)

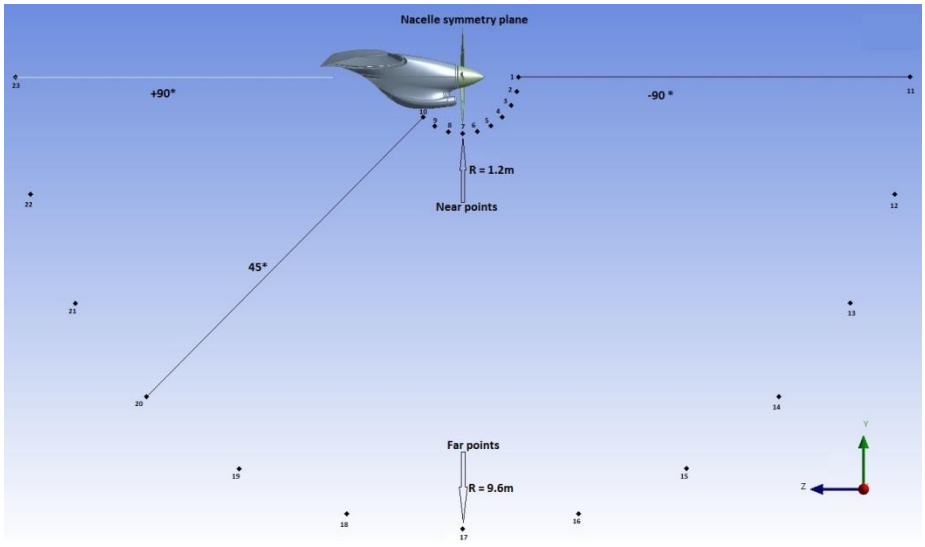

Fig. 4. – Locations of points in the near field and far field, with an increment of 15°

4. NUMERICAL RESULTS

The aerodynamic and aeroacoustic sources and noise have been computed using Ansys – Fluent. The flow condition chosen represents the "climb after take-off" condition and it translates into:

- Propeller Rotational speed: 2200 RPM
- Altitude: 0m
- Temperature: ISA + 0°C
- Speed: 130km/h TAS
- Aircraft Angle of Attack: 7°
- Engine Inlet Mass-flow Rate: 2.4 kg/s.

The flow field is computed first for the steady state with a fixed mesh, the propeller rotation is modelled by rotating the reference frame of the domain that contains it. This steady state is taken as the initial condition for the unsteady solver.

The unsteady solver this time uses the sliding mesh technique to rotate the propeller at the imposed rotational speed. To exchange information in between domains special interfaces are modeled.

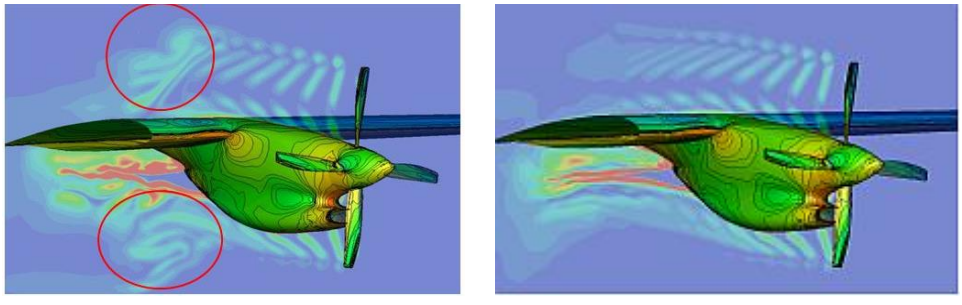

Flow solution after 1.5 revolutions Flow solution after 3.5 revolutions

Fig. 5. – Vorticity field in the median plane. Pressure contours on the surface

The flow field after 3-4 revolutions is free from the unphysical solution, that is present at t =1.5 revolutions, due to the initialization and sudden start of the rotation.

The wake vortices are dissipated far after the propeller due to the increase in grid size. Therefore after 4 complete revolutions the FWH acoustic solver is set to monitor for acoustic sources on solid surfaces that form the blades + spinner and the nacelle.

Supplementary to this another ten sources (points 1 to 10 in the table above) in the near field are set up to monitor the unsteady pressure fluctuation to allow us to compute the sound in a direct manner.

This is run for another 2-3 revolutions to build a database for the acoustics. Points 1-10 in the near field correspond radially to points 11-23 respectively in the far field.

The FWH solver by monitoring only solid surfaces as sources takes into account only monopoles and dipoles. The results obtained with the DSC and the FWH analogy are presented hereafter.

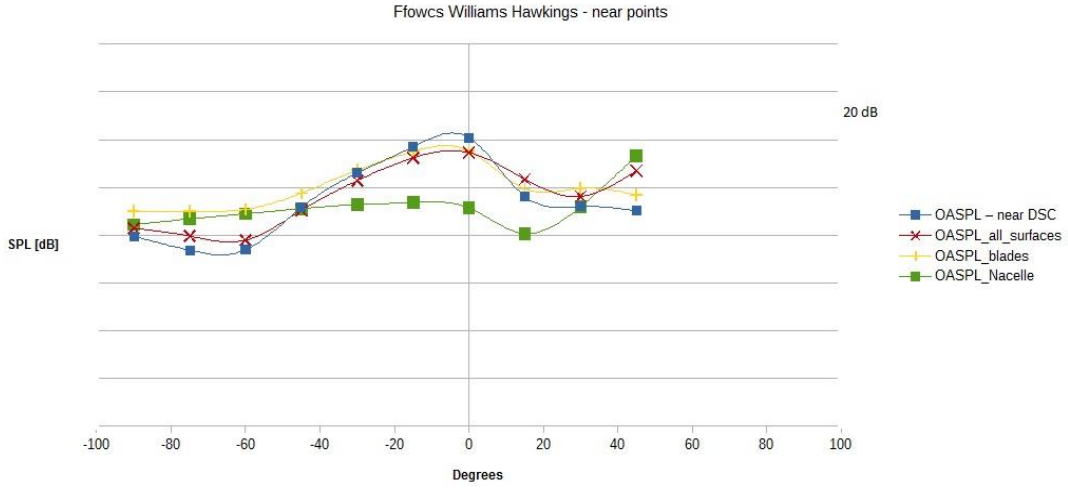

Fig. 6. - Validation of DSC with FWH on near points

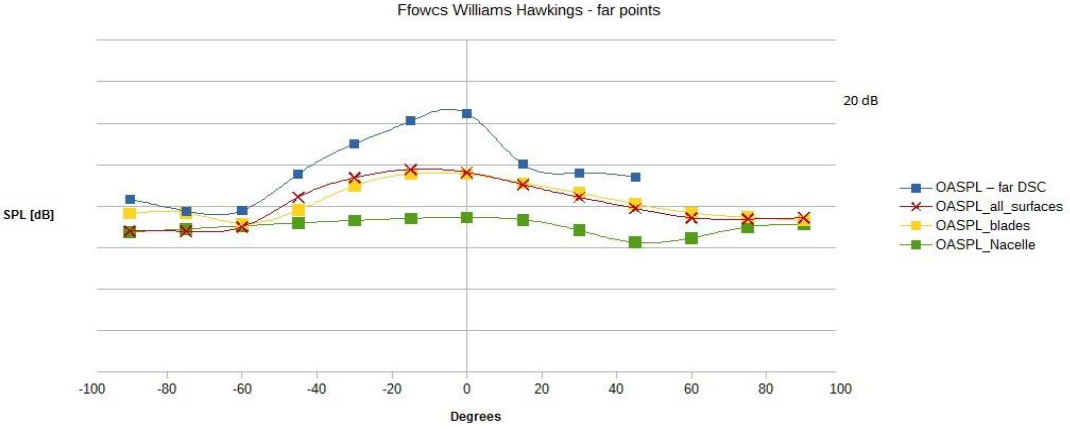

Fig. 7. - Different acoustic sources noise levels at far points and their respective contributions to OASPL FWH method

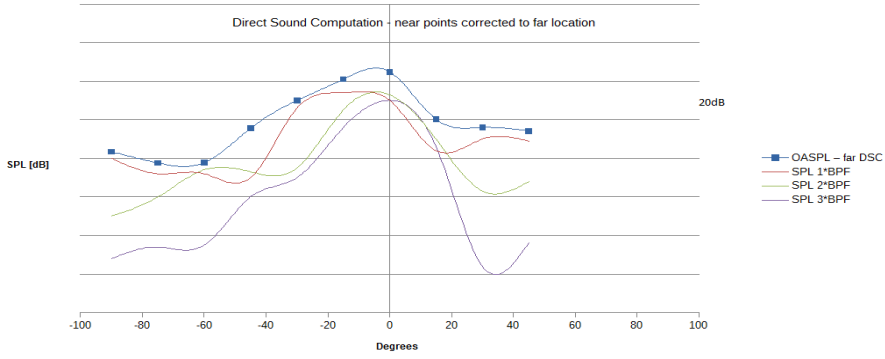

Fig. 8. - Frequency-by-frequency analysis on the far points. DSC method

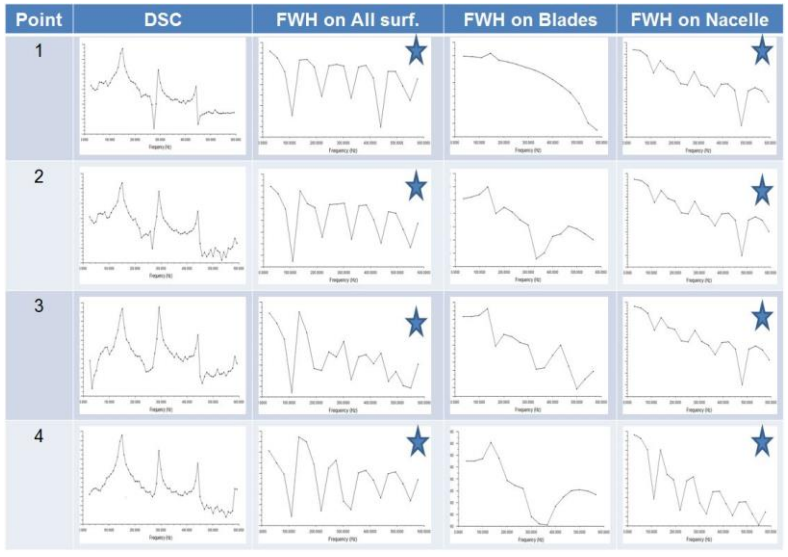

Fig. 9. – Sound Pressure Levels of the near points. DSC and FWH method

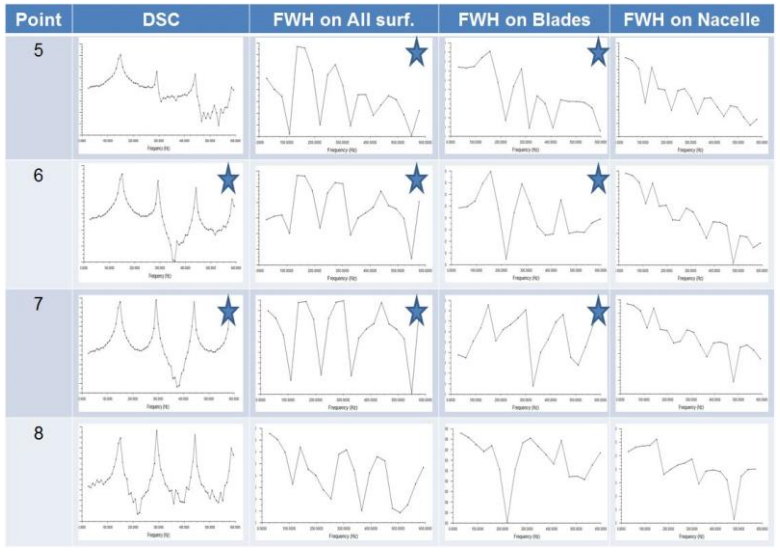

Fig. 10. - Sound Pressure Levels of the near points. DSC and FWH method

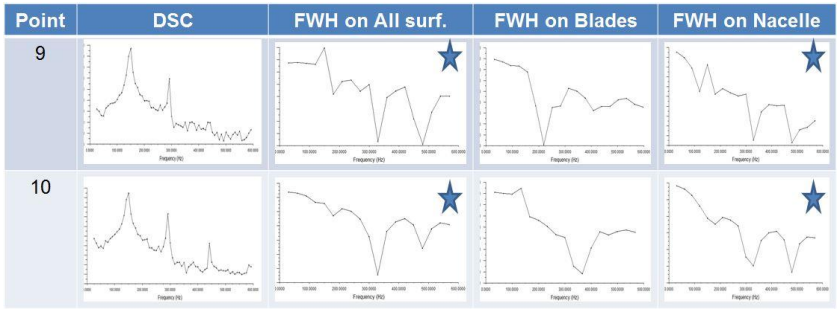

Fig. 11. - Sound Pressure Levels of the near points. DSC and FWH method

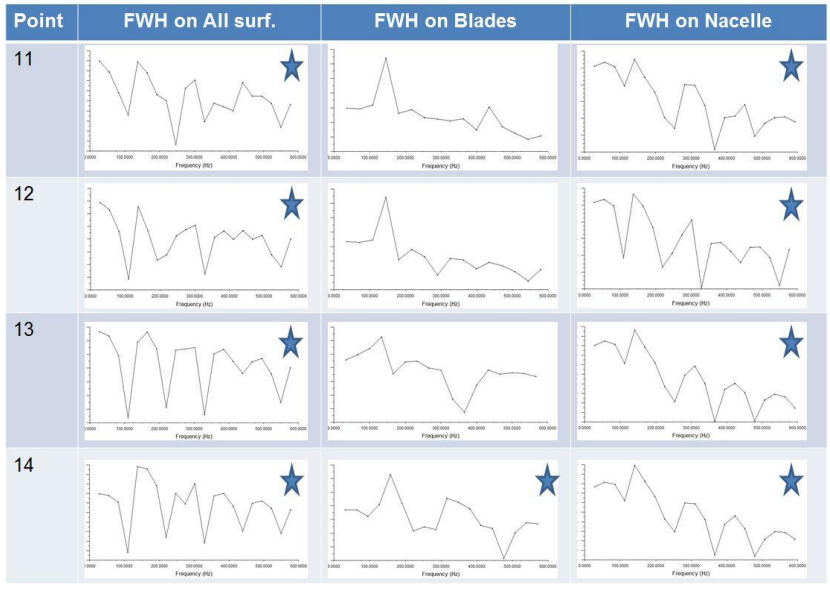

Fig. 12. - Sound Pressure Levels of the far points. FWH method

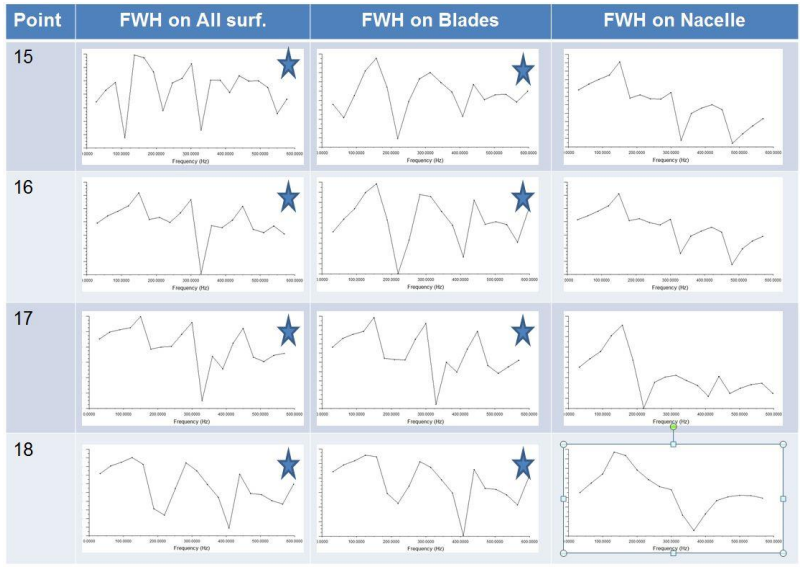

Fig. 13. - Sound Pressure Levels of the far points. FWH method

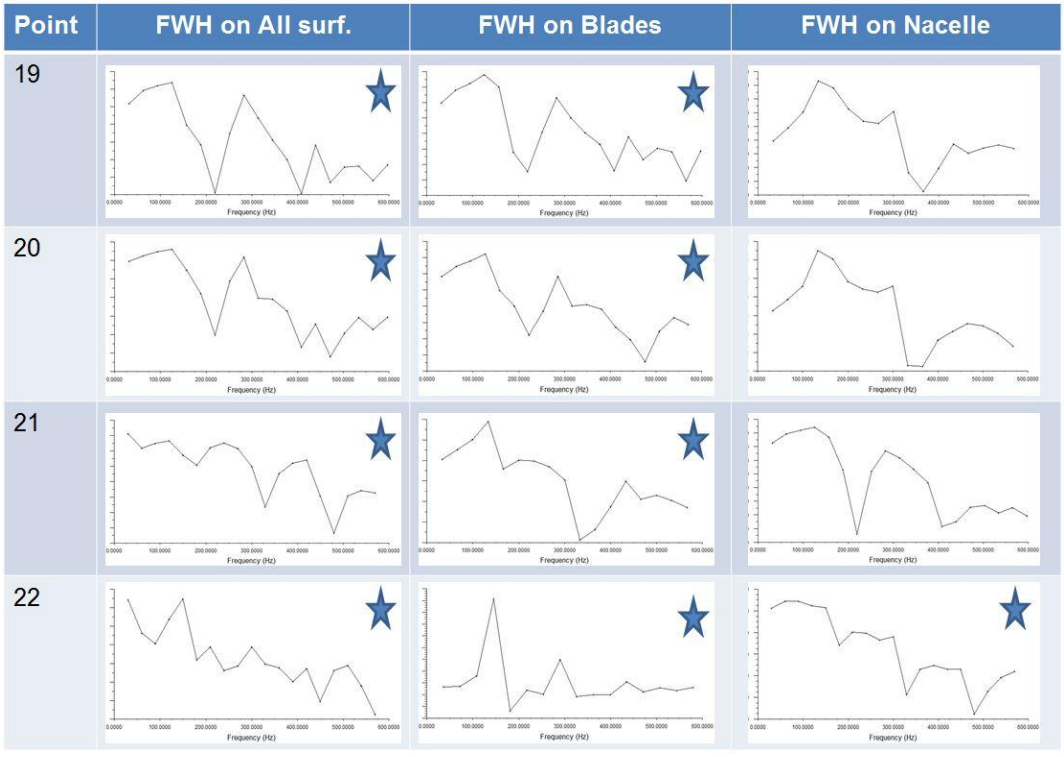

Fig. 14. - Sound Pressure Levels of the far points. FWH method

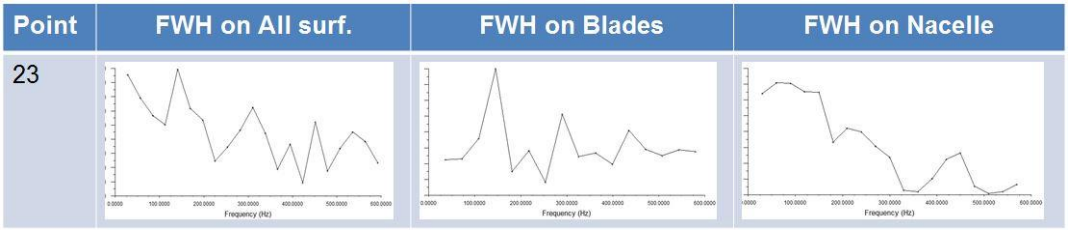

Fig. 15. - Sound Pressure Levels of the far points. FWH method

5. CONCLUSIONS

The paper presented two methods of computing the installation effects of a general aviation turboprop engine and propeller.

Noise generated by the propeller blades dominates bellow the propeller, while in front of the propeller the up to -45° the noise is due to the installation effects. Nacelle generated noise manifests itself in the near points 1, 2, 3, 4 & 9, 10 and on the far points 11, 12, 13, 14 & 22, 23. Noise on points 1, 2, 3, 4 & 11, 12, 13, 14 is generated by interaction of propeller induced perturbations that reflect on the nacelle. Elevated noise of points 9 & 10 could be due to jet noise.

Both methods provide a good agreement amongst themselves and the FWH method could have improved results if the inclusion of quadrupoles as acoustic sources will be performed. This can be done simply by using a permeable surface around the blades as monitor for acoustic sources.

REFERENCES

[1] O. Labbe, C. Peyret, G. Rahier. M. Huet, A CFD/CAA coupling method applied to jet noise prediction, *Computers and fluids*, vol. **86**, pp 1-13, 2013.
[2] A. Filippone, Aircraft noise prediction, *Progress in Aerospace Sciences*, vol. **86**, pp. 27-63, 2014.
[3] A. Giaque, B. Ortun, B. Rodriguez, B. Caruelle, Numerical error analysis with application to transonic propeller aeroacoustics, *Computers and Fluids*, vol. **69**, pp. 20-34, 2012.
[4] G. Bennett, J. Kennedy, C. Meskell, M. Carley, P. Jordan, H. Rice, Aeroacoustic research in Europe: The CEAS-ASC report 2013 highlights, *Journal of Sound and Vibration*, vol. **340**, pp. 39-60, 2015.
[5] J. Yin, A. Stuermer, M. Aversano, *Coupled uRANS and FW-H Analysis of Installed Pusher Propeller Aircraft Configurations*, 15-th AIAA Aeroacoustics Conference, 2009.
[6] * * * Ansys Fluent Theory Guide, release 15, 2013.
[7] * * * Ansys Fluent User's Guide, release 15, 2013.